Delocalization Transition of a Disordered Axion Insulator

Zhi-Da Song, Biao Lian, Raquel Queiroz, Roni Ilan, B. Andrei Bernevig, and Ady Stern

Phys. Rev. Lett. **127**, 016602 — Published 29 June 2021

DOI: 10.1103/PhysRevLett.127.016602

Delocalization Transition of Disordered Axion Insulator

Zhi-Da Song,[1,*] Biao Lian,[1] Raquel Queiroz,[2] Roni Ilan,[3] B. Andrei Bernevig,[1,4,5] and Ady Stern[2,†]

[1] *Department of Physics, Princeton University, Princeton, New Jersey 08544, USA*
[2] *Department of Condensed Matter Physics, Weizmann Institute of Science, Rehovot 7610001, Israel*
[3] *Raymond and Beverly Sackler School of Physics and Astronomy, Tel Aviv University, Tel Aviv 69978, Israel*
[4] *Physics Department, Freie Universitat Berlin, Arnimallee 14, 14195 Berlin, Germany*
[5] *Max Planck Institute of Microstructure Physics, 06120 Halle, Germany*

(Dated: April 29, 2021)

The axion insulator is a higher-order topological insulator protected by inversion symmetry. We show that under quenched disorder respecting inversion symmetry *on average*, the topology of the axion insulator stays robust, and an intermediate metallic phase in which states are delocalized is unavoidable at the transition from an axion insulator to a trivial insulator. We derive this conclusion from general arguments, from classical percolation theory, and from the numerical study of a 3D quantum network model simulating a disordered axion insulator through a layer construction. We find the localization length critical exponent near the delocalization transition to be $\nu = 1.42 \pm 0.12$. We further show that this delocalization transition is stable even to weak breaking of the average inversion symmetry, up to a critical strength. We also quantitatively map our quantum network model to an effective Hamiltonian and we find its low energy k·p expansion.

Introduction Localization of electronic states in disordered systems has been extensively studied in the past decades [1, 2]. In particular, studies on the quantum Hall states reveal a profound relation between delocalization and the topology of the electronic state [3–6]. Hence an interesting question is how the localization interplays with the full range of band topologies discovered in the past two decades. For topological insulators [7–13] protected by nonspatial symmetries [14, 15], it has been shown that the gapless boundary states are stable against symmetry-respecting disorder [13, 16–20], and the phase transition point between phases of different bulk topological numbers has protected extended bulk states at the chemical potential [6, 21, 22]. Topological states protected by translation [23, 24] or mirror [21, 25] symmetries are shown to have stable gapless surface states if the crystalline symmetries are respected on average by the disorder. However, such analyses do not explore the effect of disorder on bulk states, and do not generalize to the topological states protected by generic crystalline symmetries [26–31], such as higher-order topological insulators [32–39]. Very recently, some numerical studies have shown the robustness of the higher-order topological insulators [40–43], but an understanding of this robustness and of the delocalization transitions of these insulators is still lacking.

In this work, we focus on bulk delocalization transitions of a disordered axion insulator [28, 44–46], which is recently identified as a higher-order topological insulator protected by inversion symmetry [32, 47–51]. We show that a 3D delocalized metallic phase necessarily arises during the transition from an axion insulator to a trivial insulator as long as the inversion symmetry is respected (or broken weakly enough) on average. Such a delocalization transition manifests the robustness of the axion insulator topology against disorder.

Layer construction argument We consider a 3D crystal with inversion symmetry that maps $(x, y, z) \to (-x, -y, -z)$ and translation symmetry that maps $(x, y, z) \to (x + t_x, y + t_y, z + t_z)$, with $t_{x,y,z} \in \mathbb{Z}$ (Fig. 1c). A shifted inversion operation centered at $(t_x/2, t_y/2, t_z/2)$ consists of the combination of inversion and translation. There are eight shifted inversion centers in each unit cell, corresponding to $t_{x,y,z} = \{0, 1\}$, respectively. Ref. [52] shows that the axion insulator state can be constructed from weakly coupled Chern insulators sublayers [53–56] occupying the inversion centers, where for the A sublayers at $z = 0, \pm 1 \cdots$ the Chern number is $C = 1$ and for the B sublayers at $z = \pm\frac{1}{2}, \pm\frac{3}{2} \cdots$ it is $C = -1$ (Fig. 1c). The net Chern number in each unit cell is zero. The topology of the axion insulator relies on the fact that one cannot trivialize the construction without breaking inversion symmetry. For example, dimerizing each sublayer A at $z \in \mathbb{Z}$ with the sublayer B at either $z + \frac{1}{2}$ or $z - \frac{1}{2}$ leads to a trivial insulator, but breaks the inversion symmetry (Fig. 1d).

Our analysis starts from 2D. We consider a slab made of a finite odd number of layers $N_z \gg 1$ and a very large number of unit cells in the x, y directions, $N_{x,y} \gg N_z$. Topologically the slab is a 2D Chern insulator, say of $C = 1$. Hence the $x - z$ and $y - z$ sides host chiral modes. Weak disorder localizes all bulk states except states close to two critical energies $E_{c,1}, E_{c,2}$, one per band. The delocalized states couple the chiral modes on opposite sides, thus allowing a transition between different values of the Chern number. Assuming that the disorder is uniformly distributed within the system, we conclude that the delocalized bulk states are delocalized in all three dimensions in the slab. As disorder gets stronger, $E_{c,1}$ and $E_{c,2}$ get closer to one another, until at some critical disorder they become equal, and the system turns trivial at all energies

* zhidas@princeton.edu
† adiel.stern@weizmann.ac.il

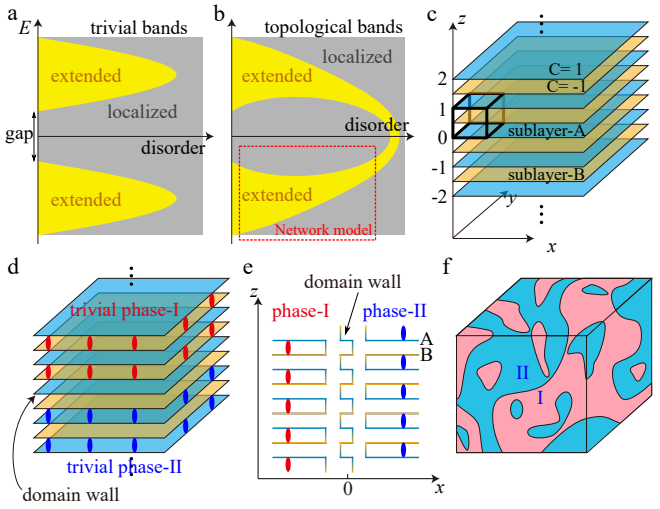

FIG. 1. Localization and band topology. (a-b) Localized (grey) and delocalized (yellow) regions in the spectrum as a function of disorder for 3D trivial and axion insulators, respectively. (c) Layer construction for the axion insulator, where the black box denotes the 3D unit cell. Sublayers A (blue) and B (orang) are decorated by 2D Chern insulators with Chern numbers $C = 1, -1$, respectively. Each unit cell has eight inversion centers $(t_x/2, t_y, t_z)$ $(t_{x,y,z} = 0, 1)$, all of which lie in a Chern layer. (d) Two possible inversion-breaking dimerized phases (I and II), which are inversion partners. (e) Side view of the domain wall in the xz direction. (f) A disordered axion insulator with random dimerizations, where the red and blue regions represent phases I and II, respectively. The domain walls between phases I and II are Chern layers and host extended states.

[3–6]. (See Ref. [57] for more discussions.)

Now we approach the 3D limit, making N_x, N_y, N_z all very large and comparable to one another. As long as N_z is odd (required by inversion symmetry) and the chemical potential is tuned properly, the Chern number is $C = 1$, there still is a chiral gapless mode encircling the sample on the side surfaces, and there would still be bulk delocalization transition as a function of energy and disorder. We expect that the critical energies $E_{c,1}$ and $E_{c,2}$ develop into two energy regions of extended states, as shown in Fig. 1b.

This analysis relies on inversion symmetry: If the inversion is broken, *e.g.*, two layers within each unit cell are dimerized, each dimerized pair becomes a trivial insulator, in which disorder localizes all states. The Chern transition is then confined to one unpaired 2D layer.

While this analysis is based on the Chern number that the system carries for an odd N_z, the thermodynamic 3D limit should not depend on the parity of N_z. Adding an additional $C = -1$ layer to the system will not change the localization properties, because the extra layer applies a local perturbation, while the delocalized states are extensive. Thus, the delocalized states occurring at the band gap at a critical disorder strength will remain even in the absence of a Chern number, and will signify the transition from an axion to a trivial insulator.

In order to form a physical picture of this transition we define two inversion-breaking dimerized phases (Fig. 1d): (I) where sublayer A at $z \in \mathbb{Z}$ couples with sublayer B at $z - \frac{1}{2}$, and (II) where sublayer A at $z \in \mathbb{Z}$ couples with sublayer B at $z + \frac{1}{2}$. Phase-I and phase-II are inversion partners, and the domain wall between them is a Chern insulator layer. The domain wall does not have to be perpendicular to z-direction (see Ref. [57] and Fig. 1e). Inversion-breaking disorders can then be simulated by placing random dimerizations in the 3D bulk, so that the bulk randomly forms phase-I and phase-II in different regions (Fig. 1e). When the volume fractions of phase-I and phase-II are equal, we say inversion symmetry is respected on average. We have only considered dimerization disorder for simplicity. More complicated disorder configurations do not change the conclusion [57].

Since each domain wall hosts a 2D Chern insulator with $C = \pm 1$, it must host 2D delocalized states at the energy of a delocalization transition. If the domain walls form an infinitely large cluster, the extended states extends over the 3D bulk. Then, when the chemical potential is at the energies of these extended states, a 3D delocalization transition happens to a trivial insulator phase. On the contrary, if the domain walls do not extend to infinity, the disordered axion insulator and trivial insulator would be connected without phase transition. By the classical 3D continuum percolation theory [58], the domain walls extend to infinity if the volume fraction p_1 of phase-I (or $p_2 = 1 - p_1$ of phase-II) is between 0.17 and 0.83. Therefore, we expect 3D delocalization transition to exist if inversion symmetry is respected on average ($p_1 = 0.5$) or broken weakly enough ($0.17 < p_1 < 0.83$).

Quantum network model Our classical percolation argument neglects quantum tunneling between neighboring domain walls. To verify the existence of delocalization transition, we study a disordered 3D quantum network model for the layer-constructed axion insulator, which describes Anderson transition with respect to changing chemical potential. The model includes only one band for each layer, and is thus suitable for a transition taking place within that band (Fig. 1b). Its analysis also demonstrates the effect of inversion symmetry breaking on this transition.

In the decoupled layers limit, each sublayer forms a 2D Chalker-Coddington quantum Hall network model [5] (Fig. 2a-b). For convenience, here we shift the inversion centers to $(t_x/2, t_y/2, \frac{1}{4} + t_z/2)$ $(t_{x,y,z} = 0, 1)$ such that the Chern layers are in the $z = \frac{1}{4}$ and $z = \frac{3}{4}$ planes. The blue (orange) and empty regions in sublayer A (B) have $C = 1$ ($C = -1$) and $C = 0$, respectively, while the red lines represent the chiral edge modes. The amplitude ψ_i of a chiral mode propagating through a bond i gains a (quenched) random propagation phase $e^{i\phi_i}$. Two chiral modes are coupled by tunneling at the crossings of the red lines. As shown in Fig. 2b, the two outgoing modes (ψ_2, ψ_4) are scattered from the two incoming

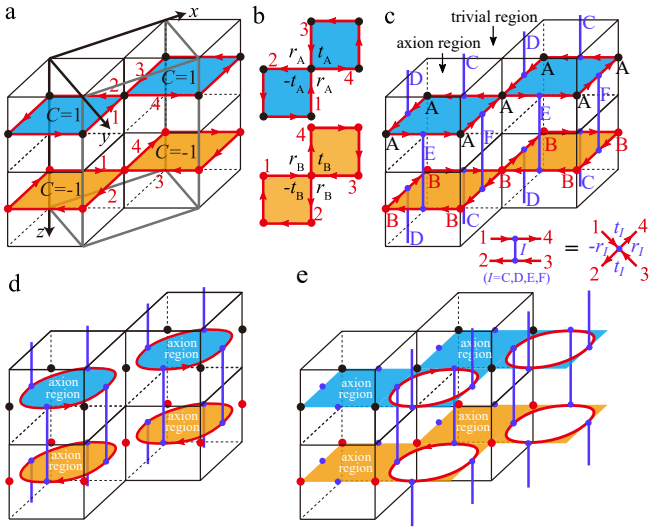

FIG. 2. The quantum network model for the axion insulator. (a) A side view of the 3D system. The blue (orange) regions have a Chern number 1 (-1). The grey box represents the repeating unit. The inversion centers are at $(t_x/2, t_y/2, \frac{1}{4} + t_z/2)$ for $t_{x,y,z} = 0, 1$. The red lines with arrows are the chiral modes surrounding the Chern regions. (b) Scatterings at the single-layer level. Here $t_{A,B}$ and $r_{A,B}$ are the transmission and reflection amplitudes of the scattering, respectively. (c) Introducing inter-layer scatterings. The nodes C, D (E, F) scatters the edge states in the blue layer to the edge states in the orange layer in the above (below). (d-e) The localized edge states of the Chern regions in the trivial ($t_{A,B} = 1$) and axion insulator ($t_{A,B} = 0$) limits, respectively.

modes (ψ_1, ψ_3) as

$$\psi_2 = -t_{A,B}\psi_1 + r_{A,B}\psi_3, \qquad \psi_4 = r_{A,B}\psi_1 + t_{A,B}\psi_3, \quad (1)$$

where $t_{A,B} = \cos\theta_{A,B}$ and $r_{A,B} = \sin\theta_{A,B}$ are referred to as the transmission and reflection amplitudes in sublayer A and B, respectively, which we assume are spatially uniform. We choose $t_{A,B}$ and $r_{A,B}$ as real numbers because we can absorb their phases into the propagating phases ϕ_i. The sublayers go through a phase transition from $C = \pm 1$ at $\frac{\pi}{4} < \theta_{A,B} \leq \frac{\pi}{2}$ to $C = 0$ at $0 \leq \theta_{A,B} < \frac{\pi}{4}$ [5, 57]. At the single energy $\theta_{A,B} = \frac{\pi}{4}$, states in each layer are delocalized.

The decoupled layers limit is inversion symmetric without disorder, *i.e.*, with spatially uniform propagation phases ϕ_i. Looking at the system as 3D, the pillars (Fig. 2c) containing the colored regions of sublayers A or B are regions of axion insulators. while the complementary empty regions are trivial insulator regions. We emphasize that there is no explicit relation between the axion or trivial regions and the phase-I or phase-II shown in Fig. 1. Both the axion regions and trivial regions are centrosymmetric by themselves, while phase-I and phase-II transform to each other under the inversion. Turning on the disorder (randomness in phases ϕ_i) breaks inversion symmetry, but preserves it on average when the ϕ_i are uniformly random.

We introduce inter-layer scattering nodes at the midpoints of each square, half way between the intra-layer ones, represented by blue vertical lines in Fig. 2c-e. On each square there are four scattering nodes. Nodes of the C, D types couple blue layer edge modes to the orange layer edge modes in the layer above, while E, F types couple the blue layer edge modes to the layer below. We parametrize the transmission and reflection amplitudes in the nodes $t_I = \cos\theta_I$ and $r_I = \sin\theta_I$ $(I = C, D, E, F)$, respectively. More details of the scattering parameters are given in Fig. S1 in Ref. [57]. We use four variables $\mu, \gamma, \eta, \delta$ to parameterize the angles:

$$\theta_A = \frac{\pi}{4} + \mu - \eta, \qquad \theta_B = \frac{\pi}{4} + \mu + \eta, \quad (2)$$

$$\theta_C = \theta_D = \gamma(1-\delta), \qquad \theta_E = \theta_F = \gamma(1-\delta) + \delta\frac{\pi}{2}, \quad (3)$$

μ can be interpreted as the chemical potential, η tunes the potential energy difference between two sublayers, γ and δ determine the inter-layer couplings. Inversion transforms the nodes C, D to E, F, respectively (Fig. 2), and therefore inversion symmetry is broken on average when δ is non-zero. We set $\gamma = \pi/8$ in the rest of this work such that the inter-layer coupling is weak compared to the intra-layer couplings. As explained in the following paragraphs, the insulating limits are independent with γ, hence the choice of γ does not qualitatively change the phase diagram of the quantum network model.

We now study the delocalization transitions with respect to the chemical potential (μ), the potential difference between two layers (η), and the inversion symmetry breaking (δ). For an inversion symmetric (on-average) system $\eta = \delta = 0$. The sublayers are either both trivial or both topological. When $\mu = -\frac{\pi}{4}$, one has $t_{A,B} = 1$, and the chiral modes surrounding the $C = \pm 1$ regions are closed in each layer and but are vertically connected to the closed chiral modes in the nearby layers (Fig. 2d). The axion regions can then be adiabatically shrank to zero, so the 3D bulk is in the trivial insulator phase. When $\mu = \frac{\pi}{4}$, the chiral modes flow surrounding the trivial regions ($t_{A,B} = 0$) as shown in Fig. 2e, so the 3D bulk is in the axion insulator phase. In this case, each Chern layer contributes to a chiral mode on the side surface of the system. Therefore, tuning μ from $-\frac{\pi}{4}$ to $\frac{\pi}{4}$ tunes the chemical potential from the bottom to the top of the topological bands of the axion insulator (Fig. 1b). In particular, when $\mu = 0$, $\theta_{A,B}$ are equal to $\pi/4$, and the 3D bulk must be delocalized because the chiral modes form a connected network, corresponding to the region of delocalized states in Fig. 1b.

In contrast, varying η from 0 to $\pi/4$ for $\mu = \delta = 0$, each sublayer A becomes a trivial insulator $(\theta_A = 0)$, while each sublayer B becomes a Chern insulator with $C = -1$ $(\theta_B = \frac{\pi}{2})$. Therefore, η drives the system into a 3D QAH insulator.

Finally, we consider strong inversion symmetry breaking. When $\delta = 1$, there is $t_C = t_D = 1$, $t_E = t_F = 0$, and

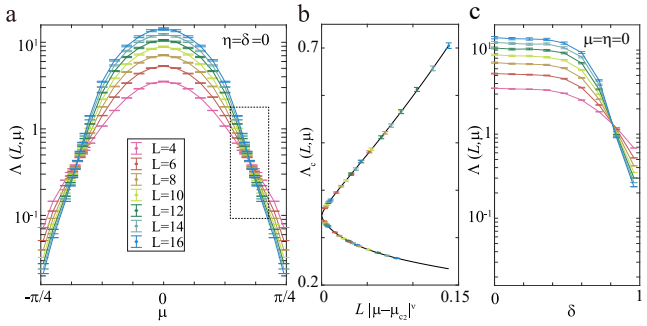

FIG. 3. Numerical results. (a) The normalized localization length Λ of the quasi-1D system is plotted as a function of μ at different system sizes (widths) L. The system is delocalized for μ between the two Anderson transition points $\mu_c \approx \pm 0.56$. (b) shows the one-parameter scaling of the relevant part of Λ around $\mu \approx 0.56$. The two branches correspond to $\mu > 0.56$ and $\mu < 0.56$, respectively. (c) shows the localization transition of Λ due to the inversion symmetry breaking on average, where δ tunes the symmetry breaking strength.

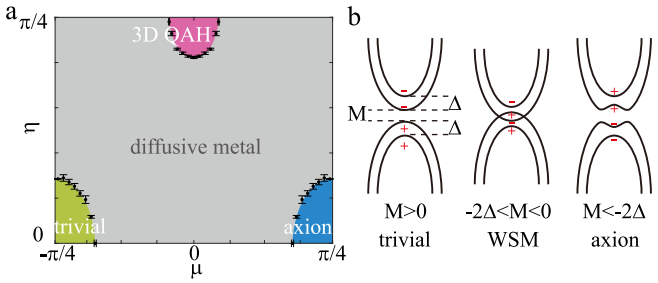

FIG. 4. Disordered topological phases. (a) Phase diagram in the parameter space of μ and η. δ is set to zero. (b) Gap closing transition from trivial insulator to axion insulator. The $\pm$ symbols represent the parities of the Bloch states.

hence a blue layer is decoupled from the orange layer above it but is fully coupled to the orange layer below it. The 3D network decomposes into disconnected 2D slices in the z-direction. Since each slice has a vanishing Chern number, there is no guaranteed delocalized state. Therefore, no delocalization transition with respect to μ is expected if $\delta = 1$. See Ref. [57] for more details.

Numerical results The localization length of the network model can be computed with a quasi-1D geometry [5, 59, 60]. Technical details are in Ref. [57]. A quasi-1D system is always localized, with the localization length depending on the transverse dimension L. The object of interest is the normalized localization length $\Lambda = \lambda/L$ [59, 60]. When Λ is finite or divergent in the $L \to \infty$ limit, the 3D states are delocalized.

We start with inversion symmetry satisfied on average, *i.e.*, $\delta = 0$. (δ is defined in Eq. (3).) For $\eta = 0$, Fig. 3a shows $\Lambda(\mu, L)$ as a function of μ and L. At $\mu = 0$, $\Lambda(\mu, L)$ increases with L, which implies 3D delocalized states. In contrast, at $\mu = \pm\frac{\pi}{4}$, $\Lambda(\mu, L)$ decreases with L and approaches zero as $L \to \infty$, implying localized states. As we discussed earlier in Fig. 2, $\mu = -\frac{\pi}{4}$ and $\mu = \frac{\pi}{4}$ correspond to the trivial insulator and axion insulator phases, respectively. Fig. 3a indicates that there is a delocalized metallic phase between them with the two delocalization Anderson transitions happening at $\mu_c \approx \pm 0.56$, where $\Lambda(\mu, L)$'s for different L's cross each other.

On the insulator side of the transitions, the 3D localization length diverges as $\xi \sim |\mu - \mu_c|^{-\nu}$, with a universal exponent $\nu > 0$. For sufficiently large L, $\Lambda(\mu, L)$ is subject to the one-parameter scaling of the single parameter L/ξ [59, 60]. When L is small, $\Lambda(\mu, L)$ also contains L dependent irrelevant terms because of the finite-size effect, and assumes the following form [61]:

$$\Lambda(\mu, L) = G_0((\mu - \mu_c)L^{\frac{1}{\nu}}) + L^y G_1((\mu - \mu_c)L^{\frac{1}{\nu}}). \quad (4)$$

Here $y < 0$ is an irrelevant scaling exponent, and $G_i(x)$ $(i = 0, 1)$ are undetermined functions which we keep up to the third order. We fit the parameters by the least square method [57] for the data points in the dashed rectangular in Fig. 3a. Fig. 3b shows the relevant part $\Lambda_c = G_0$ as a function of $L|\mu - \mu_c|^\nu$. The universal exponent from our fitting is $\nu = 1.42 \pm 0.12$, which is close to that of the 3D Anderson transition under magnetic field (where ν is found 1.3 ± 0.15 [62], 1.45 ± 0.25 [63], 1.43 ± 0.04 [64], and 1.443 ± 0.006 [65]).

We have theoretically presented arguments that strong inversion symmetry breaking leads to localization and showed that in the network model $\delta = 1$ corresponds to an inversion-broken localized limit. By tuning δ in the metal phase at $\mu = \eta = 0$, we observe an Anderson transition at $\delta \approx 0.81$ to the inversion-broken localized phase (Fig. 3c).

Keeping $\delta = 0$ and applying finite-size scaling to nonzero η, which represents the potential energy difference between sublayers A and B, we obtain a phase diagram of Fig. 4a in the parameter space of μ, η with inversion symmetry respected on average. A new insulating phase arises near $\mu = 0$, $\eta = \frac{\pi}{4}$. For a clean system, at $\mu = 0$, $\eta = \frac{\pi}{4}$, sublayer A is at a $C = 0$ state and sublayer B at $C = -1$, hence this phase is a 3D QAH insulator [66].

Discussion We used here μ as the transition tuning parameter (Fig. 1). ANother possible tuning parameter is the band gap, for which the transitions happen at gap closings that change the topology of the bands (Fig. 4b). We quantitatively map the clean quantum network model to an effective Hamiltonian, where the parameter μ plays the role of gap and the diffusive metal in Fig. 4a is found to be equivalent to the Weyl semimetal [67–71] with disorder [72–74]. See Ref. [57] for more discussions. We expect the delocalization transitions to be studied in the recently proposed axion insulator materials [49–51, 75–80] in the future.

Acknowledgement We are grateful to Xiao-Yan Xu and Yuanfeng Xu for useful discussions. B. A. B. and Z.-D. S. were supported by the DOE Grant No. DE-SC0016239, the Schmidt Fund for Innovative Research,

Simons Investigator Grant No. 404513, and the Packard Foundation. Further support was provided by the NSF-EAGER No. DMR 1643312, NSF-MRSEC No. DMR-1420541, and ONR No. N00014-20-1-2303, Gordon and Betty Moore Foundation through Grant GBMF8685 towards the Princeton theory program. The development of the network model is supported by DOE Grant No. DE-SC0016239. R. I. and B. A. B. also acknowledge the support from BSF Israel US foundation No. 2018226. A. S. acknowledges supports from the European Research Council (Project LEGOTOP), the National Science Foundation under Grant No. NSF PHY-1748958, the Israel Science Foundation - Quantum Program, and the RC/Transregio 183 of the Deutsche Forschungsgemeinschaft.

Note added. We are aware of a related work [81] focusing more on the surface delocalization transition. Their results, when overlap, are consistent with ours.

[1] P. W. Anderson, "Absence of diffusion in certain random lattices," Phys. Rev. **109**, 1492–1505 (1958).

[2] Elihu Abrahams, *50 years of Anderson Localization* (world scientific, 2010).

[3] DE Khmel'nitskii, "Quantization of hall conductivity," JETP lett **38** (1983).

[4] Herbert Levine, Stephen B. Libby, and Adrianus M. M. Pruisken, "Electron delocalization by a magnetic field in two dimensions," Phys. Rev. Lett. **51**, 1915–1918 (1983).

[5] JT Chalker and PD Coddington, "Percolation, quantum tunnelling and the integer Hall effect," Journal of Physics C: Solid State Physics **21**, 2665 (1988).

[6] Andreas W. W. Ludwig, Matthew P. A. Fisher, R. Shankar, and G. Grinstein, "Integer quantum hall transition: An alternative approach and exact results," Phys. Rev. B **50**, 7526–7552 (1994).

[7] C. L. Kane and E. J. Mele, "Z_2 topological order and the quantum spin hall effect," Phys. Rev. Lett. **95**, 146802 (2005).

[8] B. Andrei Bernevig, Taylor L. Hughes, and Shou-Cheng Zhang, "Quantum spin hall effect and topological phase transition in hgte quantum wells," Science **314**, 1757–1761 (2006).

[9] Markus König, Steffen Wiedmann, Christoph Brüne, Andreas Roth, Hartmut Buhmann, Laurens W. Molenkamp, Xiao-Liang Qi, and Shou-Cheng Zhang, "Quantum spin hall insulator state in hgte quantum wells," Science **318**, 766–770 (2007).

[10] M. Z. Hasan and C. L. Kane, "Colloquium: Topological insulators," Rev. Mod. Phys. **82**, 3045–3067 (2010).

[11] Xiao-Liang Qi and Shou-Cheng Zhang, "Topological insulators and superconductors," Rev. Mod. Phys. **83**, 1057–1110 (2011).

[12] Alexei Kitaev, "Periodic table for topological insulators and superconductors," AIP Conference Proceedings **1134**, 22–30 (2009).

[13] Shinsei Ryu, Andreas P Schnyder, Akira Furusaki, and Andreas W W Ludwig, "Topological insulators and superconductors: tenfold way and dimensional hierarchy," New Journal of Physics **12**, 065010 (2010).

[14] Martin R. Zirnbauer, "Riemannian symmetric superspaces and their origin in random-matrix theory," Journal of Mathematical Physics **37**, 4986–5018 (1996).

[15] Alexander Altland and Martin R. Zirnbauer, "Nonstandard symmetry classes in mesoscopic normal-superconducting hybrid structures," Phys. Rev. B **55**, 1142–1161 (1997).

[16] Hai-Zhou Lu, Junren Shi, and Shun-Qing Shen, "Competition between weak localization and antilocalization in topological surface states," Phys. Rev. Lett. **107**, 076801 (2011).

[17] Hong-Tao He, Gan Wang, Tao Zhang, Iam-Keong Sou, George K. L Wong, Jian-Nong Wang, Hai-Zhou Lu, Shun-Qing Shen, and Fu-Chun Zhang, "Impurity effect on weak antilocalization in the topological insulator bi_2te_3," Phys. Rev. Lett. **106**, 166805 (2011).

[18] J. Chen, X. Y. He, K. H. Wu, Z. Q. Ji, L. Lu, J. R. Shi, J. H. Smet, and Y. Q. Li, "Tunable surface conductivity in bi_2se_3 revealed in diffusive electron transport," Phys. Rev. B **83**, 241304 (2011).

[19] Minhao Liu, Jinsong Zhang, Cui-Zu Chang, Zuocheng Zhang, Xiao Feng, Kang Li, Ke He, Li-li Wang, Xi Chen, Xi Dai, Zhong Fang, Qi-Kun Xue, Xucun Ma, and Yayu Wang, "Crossover between weak antilocalization and weak localization in a magnetically doped topological insulator," Phys. Rev. Lett. **108**, 036805 (2012).

[20] Jing Wang, Biao Lian, and Shou-Cheng Zhang, "Universal scaling of the quantum anomalous Hall plateau transition," Physical Review B **89**, 085106 (2014).

[21] I. C. Fulga, B. van Heck, J. M. Edge, and A. R. Akhmerov, "Statistical topological insulators," Physical Review B **89**, 155424 (2014), publisher: American Physical Society.

[22] Takahiro Morimoto, Akira Furusaki, and Christopher Mudry, "Anderson localization and the topology of classifying spaces," Phys. Rev. B **91**, 235111 (2015).

[23] Zohar Ringel, Yaacov E. Kraus, and Ady Stern, "Strong side of weak topological insulators," Physical Review B **86**, 045102 (2012).

[24] Roger S. K. Mong, Jens H. Bardarson, and Joel E. Moore, "Quantum transport and two-parameter scaling at the surface of a weak topological insulator," Phys. Rev. Lett. **108**, 076804 (2012).

[25] Liang Fu and C. L. Kane, "Topology, Delocalization via Average Symmetry and the Symplectic Anderson Transition," Phys. Rev. Lett. **109**, 246605 (2012).

[26] Liang Fu, "Topological Crystalline Insulators," Phys. Rev. Lett. **106**, 106802 (2011).

[27] Roger S. K. Mong, Andrew M. Essin, and Joel E. Moore, "Antiferromagnetic topological insulators," Physical Review B **81** (2010), 10.1103/PhysRevB.81.245209, arXiv: 1004.1403.

[28] Taylor L. Hughes, Emil Prodan, and B. Andrei Bernevig, "Inversion-symmetric topological insulators," Phys. Rev. B **83**, 245132 (2011).

[29] Robert-Jan Slager, Andrej Mesaros, Vladimir Juričić, and Jan Zaanen, "The space group classification of topological band-insulators," Nature Physics **9**, 98–102 (2013).

[30] Chao-Xing Liu, Rui-Xing Zhang, and Brian K. Van-

Leeuwen, "Topological nonsymmorphic crystalline insulators," Phys. Rev. B **90**, 085304 (2014).
[31] Chen Fang and Liang Fu, "New classes of three-dimensional topological crystalline insulators: Nonsymmorphic and magnetic," Phys. Rev. B **91**, 161105 (2015).
[32] Fan Zhang, C. L. Kane, and E. J. Mele, "Surface state magnetization and chiral edge states on topological insulators," Phys. Rev. Lett. **110**, 046404 (2013).
[33] Wladimir A. Benalcazar, B. Andrei Bernevig, and Taylor L. Hughes, "Quantized electric multipole insulators," Science **357**, 61–66 (2017).
[34] Wladimir A. Benalcazar, B. Andrei Bernevig, and Taylor L. Hughes, "Electric multipole moments, topological multipole moment pumping, and chiral hinge states in crystalline insulators," Physical Review B **96**, 245115 (2017).
[35] Frank Schindler, Ashley M. Cook, Maia G. Vergniory, Zhijun Wang, Stuart S. P. Parkin, B. Andrei Bernevig, and Titus Neupert, "Higher-order topological insulators," Science Advances **4**, eaat0346 (2018).
[36] Frank Schindler, Zhijun Wang, Maia G Vergniory, Ashley M Cook, Anil Murani, Shamashis Sengupta, Alik Yu Kasumov, Richard Deblock, Sangjun Jeon, Ilya Drozdov, *et al.*, "Higher-order topology in bismuth," Nature physics **14**, 918–924 (2018).
[37] Josias Langbehn, Yang Peng, Luka Trifunovic, Felix von Oppen, and Piet W. Brouwer, "Reflection-Symmetric Second-Order Topological Insulators and Superconductors," Physical Review Letters **119**, 246401 (2017).
[38] Zhida Song, Zhong Fang, and Chen Fang, "(d-2)-Dimensional Edge States of Rotation Symmetry Protected Topological States," Physical Review Letters **119**, 246402 (2017).
[39] Motohiko Ezawa, "Higher-order topological insulators and semimetals on the breathing kagome and pyrochlore lattices," Phys. Rev. Lett. **120**, 026801 (2018).
[40] Zixian Su, Yanzhuo Kang, Bofeng Zhang, Zhiqiang Zhang, and Hua Jiang, "Disorder induced phase transition in magnetic higher-order topological insulator: A machine learning study," Chinese Physics B **28**, 117301 (2019).
[41] Hiromu Araki, Tomonari Mizoguchi, and Yasuhiro Hatsugai, "Phase diagram of a disordered higher-order topological insulator: A machine learning study," Phys. Rev. B **99**, 085406 (2019).
[42] C. Wang and X. R. Wang, "Disorder-induced quantum phase transitions in three-dimensional second-order topological insulators," Phys. Rev. Research **2**, 033521 (2020).
[43] Chang-An Li, Bo Fu, Zi-Ang Hu, Jian Li, and Shun-Qing Shen, "Topological phase transitions in disordered electric quadrupole insulators," Phys. Rev. Lett. **125**, 166801 (2020).
[44] Andrew M. Essin, Joel E. Moore, and David Vanderbilt, "Magnetoelectric polarizability and axion electrodynamics in crystalline insulators," Phys. Rev. Lett. **102**, 146805 (2009).
[45] Rundong Li, Jing Wang, Xiao-Liang Qi, and Shou-Cheng Zhang, "Dynamical axion field in topological magnetic insulators," Nature Physics **6**, 284–288 (2010).
[46] Ari M. Turner, Yi Zhang, Roger S. K. Mong, and Ashvin Vishwanath, "Quantized response and topology of magnetic insulators with inversion symmetry," Phys. Rev. B **85**, 165120 (2012).
[47] Nicodemos Varnava and David Vanderbilt, "Surfaces of axion insulators," Phys. Rev. B **98**, 245117 (2018).
[48] Benjamin J Wieder and B Andrei Bernevig, "The axion insulator as a pump of fragile topology," arXiv preprint arXiv:1810.02373 (2018).
[49] Yuanfeng Xu, Zhida Song, Zhijun Wang, Hongming Weng, and Xi Dai, "Higher-order topology of the axion insulator $EuIn_2As_2$," Phys. Rev. Lett. **122**, 256402 (2019).
[50] Changming Yue, Yuanfeng Xu, Zhida Song, Hongming Weng, Yuan-Ming Lu, Chen Fang, and Xi Dai, "Symmetry-enforced chiral hinge states and surface quantum anomalous hall effect in the magnetic axion insulator $Bi_{2-x}Sm_xSe$ 3," Nature Physics **15**, 577–581 (2019).
[51] Dongqin Zhang, Minji Shi, Tongshuai Zhu, Dingyu Xing, Haijun Zhang, and Jing Wang, "Topological axion states in the magnetic insulator $MnBi_2Te_4$ with the quantized magnetoelectric effect," Phys. Rev. Lett. **122**, 206401 (2019).
[52] Luis Elcoro, Benjamin J Wieder, Zhida Song, Yuanfeng Xu, Barry Bradlyn, and B Andrei Bernevig, "Magnetic topological quantum chemistry," arXiv preprint arXiv:2010.00598 (2020).
[53] Zhida Song, Tiantian Zhang, Zhong Fang, and Chen Fang, "Quantitative mappings between symmetry and topology in solids," Nature Communications **9**, 3530 (2018).
[54] Zhida Song, Sheng-Jie Huang, Yang Qi, Chen Fang, and Michael Hermele, "Topological states from topological crystals," Science Advances **5**, eaax2007 (2019).
[55] Hao Song, Sheng-Jie Huang, Liang Fu, and Michael Hermele, "Topological phases protected by point group symmetry," Phys. Rev. X **7**, 011020 (2017).
[56] Sheng-Jie Huang, Hao Song, Yi-Ping Huang, and Michael Hermele, "Building crystalline topological phases from lower-dimensional states," Phys. Rev. B **96**, 205106 (2017).
[57] See supplemenatry material at ... , which includes Ref. [3–6, 20, 28, 46, 52, 59, 60, 82–86].
[58] M. B. Isichenko, "Percolation, statistical topography, and transport in random media," Rev. Mod. Phys. **64**, 961–1043 (1992).
[59] A. MacKinnon and B. Kramer, "One-Parameter Scaling of Localization Length and Conductance in Disordered Systems," Phys. Rev. Lett. **47**, 1546–1549 (1981).
[60] A MacKinnon and B Kramer, "The scaling theory of electrons in disordered solids: Additional numerical results," Zeitschrift für Physik B Condensed Matter **53**, 1–13 (1983).
[61] Keith Slevin and Tomi Ohtsuki, "Corrections to Scaling at the Anderson Transition," Physical Review Letters **82**, 382–385 (1999), publisher: American Physical Society.
[62] M. Henneke, B. Kramer, and T. Ohtsuki, "Anderson Transition in a Strong Magnetic Field," Europhysics Letters (EPL) **27**, 389–394 (1994), publisher: IOP Publishing.
[63] J. T. Chalker and A. Dohmen, "Three-Dimensional Disordered Conductors in a Strong Magnetic Field: Surface States and Quantum Hall Plateaus," Physical Review Letters **75**, 4496–4499 (1995).
[64] Keith Slevin and Tomi Ohtsuki, "The anderson transition: Time reversal symmetry and universality," Phys. Rev. Lett. **78**, 4083–4086 (1997).
[65] Keith Slevin and Tomi Ohtsuki, "Estimate of the critical

exponent of the anderson transition in the three and four-dimensional unitary universality classes," Journal of the Physical Society of Japan **85**, 104712 (2016).

[66] Rui Yu, Wei Zhang, Hai-Jun Zhang, Shou-Cheng Zhang, Xi Dai, and Zhong Fang, "Quantized Anomalous Hall Effect in Magnetic Topological Insulators," Science **329**, 61–64 (2010).

[67] A. Burkov and Leon Balents, "Weyl Semimetal in a Topological Insulator Multilayer," Physical Review Letters **107**, 127205 (2011).

[68] Xiangang Wan, Ari Turner, Ashvin Vishwanath, and Sergey Savrasov, "Topological semimetal and Fermi-arc surface states in the electronic structure of pyrochlore iridates," Physical Review B **83**, 205101 (2011).

[69] Hongming Weng, Chen Fang, Zhong Fang, B. Andrei Bernevig, and Xi Dai, "Weyl Semimetal Phase in Noncentrosymmetric Transition-Metal Monophosphides," Physical Review X **5**, 011029 (2015).

[70] B. Q. Lv, H. M. Weng, B. B. Fu, X. P. Wang, H. Miao, J. Ma, P. Richard, X. C. Huang, L. X. Zhao, G. F. Chen, Z. Fang, X. Dai, T. Qian, and H. Ding, "Experimental discovery of weyl semimetal taas," Phys. Rev. X **5**, 031013 (2015).

[71] Su-Yang Xu, Ilya Belopolski, Nasser Alidoust, Madhab Neupane, Guang Bian, Chenglong Zhang, Raman Sankar, Guoqing Chang, Zhujun Yuan, Chi-Cheng Lee, Shin-Ming Huang, Hao Zheng, Jie Ma, Daniel S. Sanchez, BaoKai Wang, Arun Bansil, Fangcheng Chou, Pavel P. Shibayev, Hsin Lin, Shuang Jia, and M. Zahid Hasan, "Discovery of a Weyl Fermion semimetal and topological Fermi arcs," Science , aaa9297 (2015).

[72] Koji Kobayashi, Tomi Ohtsuki, Ken-Ichiro Imura, and Igor F. Herbut, "Density of states scaling at the semimetal to metal transition in three dimensional topological insulators," Phys. Rev. Lett. **112**, 016402 (2014).

[73] Rahul Nandkishore, David A. Huse, and S. L. Sondhi, "Rare region effects dominate weakly disordered three-dimensional dirac points," Phys. Rev. B **89**, 245110 (2014).

[74] J. H. Pixley, David A. Huse, and S. Das Sarma, "Rare-region-induced avoided quantum criticality in disordered three-dimensional dirac and weyl semimetals," Phys. Rev. X **6**, 021042 (2016).

[75] Masataka Mogi, Minoru Kawamura, Atsushi Tsukazaki, Ryutaro Yoshimi, Kei S Takahashi, Masashi Kawasaki, and Yoshinori Tokura, "Tailoring tricolor structure of magnetic topological insulator for robust axion insulator," Science advances **3**, eaao1669 (2017).

[76] Di Xiao, Jue Jiang, Jae-Ho Shin, Wenbo Wang, Fei Wang, Yi-Fan Zhao, Chaoxing Liu, Weida Wu, Moses H. W. Chan, Nitin Samarth, and Cui-Zu Chang, "Realization of the axion insulator state in quantum anomalous hall sandwich heterostructures," Phys. Rev. Lett. **120**, 056801 (2018).

[77] Jiaheng Li, Yang Li, Shiqiao Du, Zun Wang, Bing-Lin Gu, Shou-Cheng Zhang, Ke He, Wenhui Duan, and Yong Xu, "Intrinsic magnetic topological insulators in van der waals layered $MnBi_2Te_4$-family materials," Science Advances **5**, eaaw5685 (2019).

[78] Yan Gong, Jingwen Guo, Jiaheng Li, Kejing Zhu, Menghan Liao, Xiaozhi Liu, Qinghua Zhang, Lin Gu, Lin Tang, Xiao Feng, Ding Zhang, Wei Li, Canli Song, Lili Wang, Pu Yu, Xi Chen, Yayu Wang, Hong Yao, Wenhui Duan, Yong Xu, Shou-Cheng Zhang, Xucun Ma, Qi-Kun Xue, and Ke He, "Experimental realization of an intrinsic magnetic topological insulator," Chinese Physics Letters **36**, 076801 (2019).

[79] Yujun Deng, Yijun Yu, Meng Zhu Shi, Zhongxun Guo, Zihan Xu, Jing Wang, Xian Hui Chen, and Yuanbo Zhang, "Quantum anomalous hall effect in intrinsic magnetic topological insulator mnbi2te4," Science **367**, 895–900 (2020).

[80] Rui-Xing Zhang, Fengcheng Wu, and S Das Sarma, "Möbius insulator and higher-order topology in $MnBi_{2n}Te_{3n+1}$," arXiv preprint arXiv:1910.11906 (2019).

[81] Hailong Li, Hua Jiang, Chui-Zhen Chen, and XC Xie, "Critical behavior and universal signature of an axion insulator state," arXiv preprint arXiv:2010.15630 (2020).

[82] Valery Iustinovich Oseledets, "A multiplicative ergodic theorem. characteristic ljapunov, exponents of dynamical systems," Trudy Moskovskogo Matematicheskogo Obshchestva **19**, 179–210 (1968).

[83] William H. Press, *Numerical Recipes in Fortran 90: Volume 2, Volume 2 of Fortran Numerical Recipes: The Art of Parallel Scientific Computing* (Cambridge University Press, 1996).

[84] Liang Fu and C. L. Kane, "Topological insulators with inversion symmetry," Phys. Rev. B **76**, 045302 (2007).

[85] Haruki Watanabe, Hoi Chun Po, and Ashvin Vishwanath, "Structure and topology of band structures in the 1651 magnetic space groups," Science Advances **4**, eaat8685 (2018).

[86] C.-M. Ho and J. T. Chalker, "Models for the integer quantum hall effect: The network model, the dirac equation, and a tight-binding hamiltonian," Phys. Rev. B **54**, 8708–8713 (1996).